Single-shot interferometric measurement of pulse-to-pulse stability of absolute phase using a time-stretch technique

IGOR KUDELIN,[1,*] **SRIKANTH SUGAVANAM,**[1,2] **AND MARIA CHERNYSHEVA**[3]

[1]*Aston Institute of Photonic Technologies, Aston University, Birmingham, B4 7ET, UK*
[2]*School of Computing and Electrical Engineering, IIT Mandi, Kamand, Himachal Pradesh 175075, India*
[3]*Leibniz Institute of Photonic Technology, Albert-Einstein str. 9, Jena 07745, Germany*
[*]*kudelini@aston.ac.uk*

Abstract: Measurement of the absolute phase of ultrashort optical pulses in real-time is crucial for various applications, including frequency comb and high-field physics. Modern single-shot techniques, such as dispersive Fourier transform and time-lens, make it possible to investigate non-repetitive spectral dynamics of ultrashort pulses yet do not provide the information on absolute phase. In this work, we demonstrate a novel approach to characterise single-shot pulse-to-pulse stability of the absolute phase with the acquisition rate of 15 MHz. The acquisition rate, limited by the repetition rate of the used free-running mode-locked Erbium-doped fibre laser, substantially exceeds one of the traditional techniques. The method is based on the time-stretch technique. It exploits a simple all-fibre Mach-Zehnder interferometric setup with a remarkable resolution of ~7.3 mrad. Using the proposed method, we observed phase oscillations in the output pulses governed by fluctuations in the pulse intensity due to Kerr-induced self-phase modulation at frequencies peaked at 4.6 kHz. As a proof-of-concept application of the demonstrated interferometric methodology, we evaluated phase behaviour during vibration exposure on the laser platform. The results propose a new view on the phase measurements that provide a novel avenue for numerous sensing applications with MHz data frequencies.

1. Introduction

Interferometry has gained an undeniable reputation as a highly sensitive optical interrogation method for a wide range of applications in biosensing [1], gravitational wave detection [2], acoustics [3], and astronomy [4]. The heterodyne method allows achieving high resolution even for low intensities and does not require any nonlinear processes. Modern modifications of self-reference interferometry systems, such as shearing interferometry [5] or spectral interferometry for direct electric-field reconstruction (SPIDER) [6], can provide full-field pulse recovery. Nevertheless, conventional methods to record spectral information, such as optical spectrum analyser or Fourier spectrometer, limit their maximum available data frequencies.

Time-stretch techniques have enabled the investigation of non-repetitive transition dynamics of ultrashort coherent structures [7]. Among them is the Dispersive Fourier Transform (DFT), which acts as a temporal analogue of a spatial lens and performs real-time single-shot measurements in the frequency domain [8]. The DFT method has allowed experimental observation of self-organisation of ultrashort pulses [9–11], mutual soliton formation in bidirectional laser [12,13] and uncovered underlying instability dynamics such as spectral pulsations [14], soliton explosions [15] and collisions [13], and internal dynamics of soliton molecules [16]. The interference pattern, recorded by the DFT, can serve for vibration sensing [17,18] or gyroscopic [19] applications. However, time-stretch techniques are insensitive to the pulse phase, and modifications are required

to reconstruct the spectral phase profile [20,21], while the drift of the absolute phase remains unknown.

In frequency domain, the ultrashort pulse train is presented as equidistant frequency comb-lines [22]. The comb lines are separated by repetition frequency of the pulse train f_{rep} and offset from the zero by f_{CEO}. In temporal domain, f_{CEO} manifests as a pulse-to-pulse phase slip between maxima of carrier wave field and intensity envelope by $\phi_{CEO} = 2\pi f_{CEO}/f_{rep}$. Characterisation of the frequency comb, and especially f_{CEO} and carrier-envelope phase, and its control is crucial for optical frequency metrology [23], high-field physics [24] and coherent control [25]. The most established methods to measure f_{ceo} are based on complex self-referencing detection through $f - 2f$ interferometer [23] or above-threshold ionization (ATI) methods. However, the highest acquisition rate, demonstrated to date, does not exceed 100 kHz [26–28]. Moreover, these techniques involve nonlinear conversion steps (coherent octave-spanning supercontinuum and second harmonic generation), limiting applicable peak power and pulse duration. In Ref. [28] authors recorded the spectral interference from $f - 2f$ interferometer via the DFT in order to increase the acquisition rates. However, only an acquisition rate of 100 kHz was demonstrated with a potential upper limit of 10 MHz. Other works showed the possibility of retrieving the CEO phase dynamics by retrieving the relative phase between consecutive pulse from a cross-correlation [29] or interferogram [30].

In this work, we present single-shot measurements of the pulse-to-pulse changes in f_{ceo} and its short-term stability in a free-running Erbium-doped mode-locked fibre laser at a 15 MHz acquisition rate. This is the highest data rate for the CEO-phase characterisation to date. The setup comprises a simple all-fibre Mach-Zehnder interferometer with optical path difference between both arms equal to the cavity length, allowing to get the interference between consecutive pulses. The single-shot interference pattern was recorded via the DFT technique, followed by the relative phase numerical retrieval. This methodology provides a short-term (pulse-to-pulse) stability of the laser system based on phase deviation. Thus, the experiments showed 126-mrad phase deviation in the used free-running laser. The setup resolution was 7.3 mrad, which is equal to timing jitter of 6 attoseconds at a central wavelength of 1555 nm. This method allows us to reveal Kerr-induced phase oscillation at frequencies around 4.6 kHz. Finally, we show sensing capabilities of the proposed method by recovering kHz range vibrations impressed on the laser platform. We believe, these results present a novel method to characterise the short-term stability of the mode-locking lasers and can be applied in high-field physics, or acoustic vibration and temperature sensing and gyroscopic measurements at high acquisition rates.

2. Experimental methodology and setup

Fundamentally, the expression for two-pulse interference contains three parameters. The first parameter - separation between the pulses τ is encoded in the spectral fringe period $\Delta\nu = 1/\tau$. The second parameter is the absolute phase difference $\Delta\phi$ between pulses, which can be calculated as $2\pi \cdot \frac{\delta\nu}{\Delta\nu}$, where $\delta\nu$ is a spectral offset between the maximum of the fringes with respect to the spectral envelope (Figs. 1(a)–1(c)). Finally, a ratio between pulse intensities can be extracted from the modulation depths of the interference pattern.

In order to record valid data, the separation between the pulses should lie in the range defined:

$$1/\Delta\nu_{FWHM} < \tau < 1/2\nu_{res} \tag{1}$$

where, τ - time separation between the pulses, $\Delta\nu_{FWHM}$ - FWHM of the pulse spectra and ν_{res} is the resolution of the DFT. The left-hand side of the equation means that at least one modulation period should be identified in the interference pattern. The right-hand side limits the maximum pulse separation between the pulses due to the spectral resolution of the DFT technique.

Figure 1(a) shows schematically train of three pulses, whose phases are 0, 0, and π. Figures 1(b) and 1(c) demonstrate spectra of interference of N and N + 1, and N + 1 and N + 2 pulse pairs,
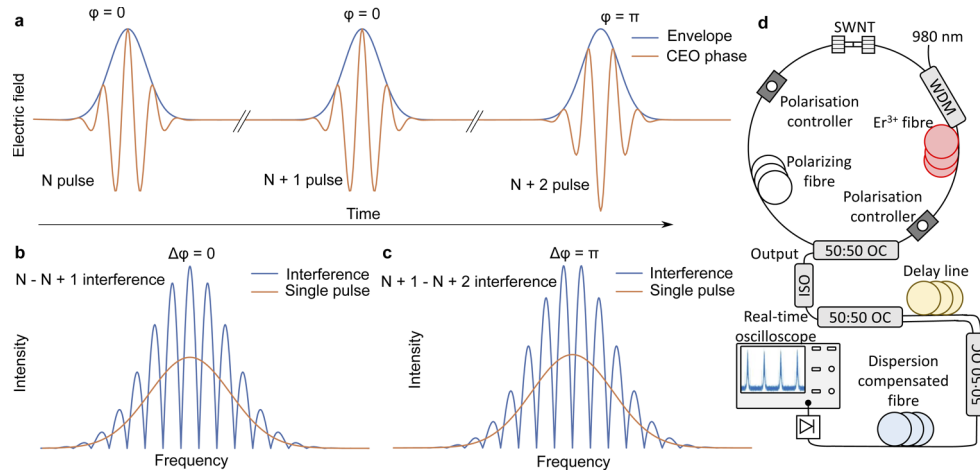
Fig. 1. (**a**) An ultrashort pulse train with the carrier and envelope. Spectrum of interference between (**b**) $N - N + 1$ and (**c**) $N + 1 - N + 2$ pulses show relative phase between pulses. (**d**) The experimental setup of mode-locked ring fiber laser for the DFT measurements. SWNT - single-walled carbon nanotubes, ISO - optical isolator, OC - optical coupler.

correspondingly. As seen in Figs. 1(b) and 1(c), such sequential spectral interferograms demonstrate carrier-envelope offset, which allows retrieval of complete phase evolution in real-time.

The erbium-doped fibre laser is detailed in work [31] and shown in Fig. 1(d). Mode-locked generation was realised by co-action of single-walled carbon nanotubes and nonlinear polarisation rotation in polarising fibre (HB1550Z from Thorlabs). The isolator-free laser configuration allows switching the directionality of mode-locked generation by adjusting polarisation controllers. For this experiment, we have enabled the unidirectional generation of 570-fs pulses with the time-bandwidth product of 0.35 in the clockwise direction at a 15-MHz repetition rate. Note that the laser fundamental repetition rate determines the maximum data acquisition frequency of the absolute phase changes. The average output power was 1 mW. The influence of the surrounding temperature fluctuations was negligible over the measured time scales. To further minimise its effect, we placed the delay line into a foam box.

Reference [30] has demonstrated that by retrieving the relative phase between consecutive pulses from the interferogram, it is possible to reconstruct the carrier-envelope phase. To enable single-shot detection of absolute phase difference at MHz-data rates, we used the DFT technique to retrieve the phase changes from consecutive pulses interference. In the current work, an all-fibre Mach–Zehnder interferometer was realised via two 3-dB fibre couplers with an additional section of SMF-28 fibre in a delay arm. The length of the delay arm of the interferometer was 13.3 m which equals the cavity length. Therefore, the leading pulse was delayed in one interferometer arm by one round-trip time. This allowed recording the interference of two consecutive pulses, similar to Figs. 1(a)–1(c). As a dispersive line for the DFT measurements, we used 11 km of dispersion compensating fibre (WBDK-70-L from OFS) with a total accumulated dispersion D = −1200 ps/nm for a signal at 1555 nm. The data were recorded by using a 50-GHz photodiode (Finisar XPDV2320R) and a 33-GHz 80-GSa/s oscilloscope (Agilent DSOX93204A), which provide a bandwidth-limited resolution of 0.021 nm [8].

3. Results

In the experiments, we have recorded 26.2 ms of consecutive interferograms, which correspond to around 390 000 round trips. Figure 2(a) demonstrates recorded single-shot spectral evolution over 1000 consecutive round trips. A typical cross-section of the DFT spectra is shown in Fig. 2(b). Strong spectral modulation, depicted in more details in the inset in Fig. 2(b), indicates persistent interference between consecutive pulses. According to the Wiener-Khinchin theorem, the Fast Fourier Transform (FFT) of the single-shot spectra provides the first-order autocorrelation function [10]. Figure 2(c) presents the corresponding 1000 round trips of field autocorrelation evolution. Figure 2(d) shows the autocorrelation function cross-section that reveals the presence of two pulses, separated by 36.5 ps. Numerically, the first-order autocorrelation function of two-pulse interference expressed as [32]:

$$R(\tau') = 2\int I_0(\omega)e^{i\omega\tau'}d\omega + e^{-i\phi}\int I_0(\omega)e^{i\omega(\tau+\tau')}d\omega + e^{i\phi}\int I_0(\omega)e^{i\omega(\tau-\tau')}d\omega \qquad (2)$$

where $I_0(\omega)$ is a spectral intensity of a single pulse, τ - time separation between pulses and ϕ is a relative phase. To estimate the resolution of the phase retrieval, CEO phase fluctuations should be not taken into consideration. Thus, an additional configuration of the Mach-Zehnder interferometer with equal arms was implemented in the experiment. In such a configuration, the pulse interferes with its own replica. Therefore, the fluctuations of the relative phase are related only to the environmental noise and uncertainty in phase retrieval. The extracted relative phase is shown in Figs. 2(e)–2(f). The standard deviation of the single-shot phase retrieval in this setup was 7.3 mrad, which equals the timing jitter of 6 attoseconds at a central wavelength of 1555 nm. This standard deviation defines the smallest distinguishable phase change from noise per round trip, which constitutes the resolution of the measurement technique.

By applying the FFT of the single-shot DFT spectra and exploiting the above-described methodology, we retrieved an overall picture of the relative phase evolution, shown in Fig. 3. Since the pulse accumulates an additional phase shift due to dispersion in the delay line of the Mach-Zehnder interferometer (0.239 ps/nm for 13 meters of SMF-28 fibre), the reference level could not be uniquely determined. Therefore, we assumed the value at the beginning of the recording as a zero reference level. In principle, the dispersion in the fibre interferometer can be compensated by implementing a dispersion-less delay line, for example, as demonstrated in [29] by using a vacuum tube.

Figure 3(a) provides information on the relative changes in the pulse phase and characterises the short-term stability of the laser. The standard deviation of the relative phase change was observed to be 126 mrad. Figure 3(b) shows a difference in the phase slip for consecutive pulses. The corresponding histogram, depicted in Fig. 3(c), obeys the normal distribution law. The standard deviation of the phase slip was 15.6 mrad, which corresponds to the timing jitter of 16.5 as at the central wavelength of 1555 nm. For results with a moving average window of $n = 15$ round trips, the standard deviation and timing jitter reduced down to 3.8 mrad and 4 as, respectively. The standard deviation decreases by $\sqrt{n}$ obeying the normal distribution. Such relation confirms the noise nature of the fluctuations in f_{CEO}.

The inset in Fig. 3(a) shows phase oscillation dynamics of the output pulses zoomed over 15 000 round trips. The observed frequency of oscillations has a peak at 4.6 kHz with 3-dB width of 570 Hz and 23 dB signal-to-noise ratio, as shown in power spectral density (PSD) in Fig. 3(d). Figure 3(e) shows the PSD of the pulse intensity derived from the interference pattern. Frequency spikes at around 4.6 kHz observed in both PSDs support our assumption that the phase oscillations were caused by the pulse energy variation due to Kerr-induced self-phase modulation [33,34]. These oscillations were mediated by active medium or pump power instabilities [35]. Note, a substantial suppression of noises at the frequency range higher than 100 kHz for the
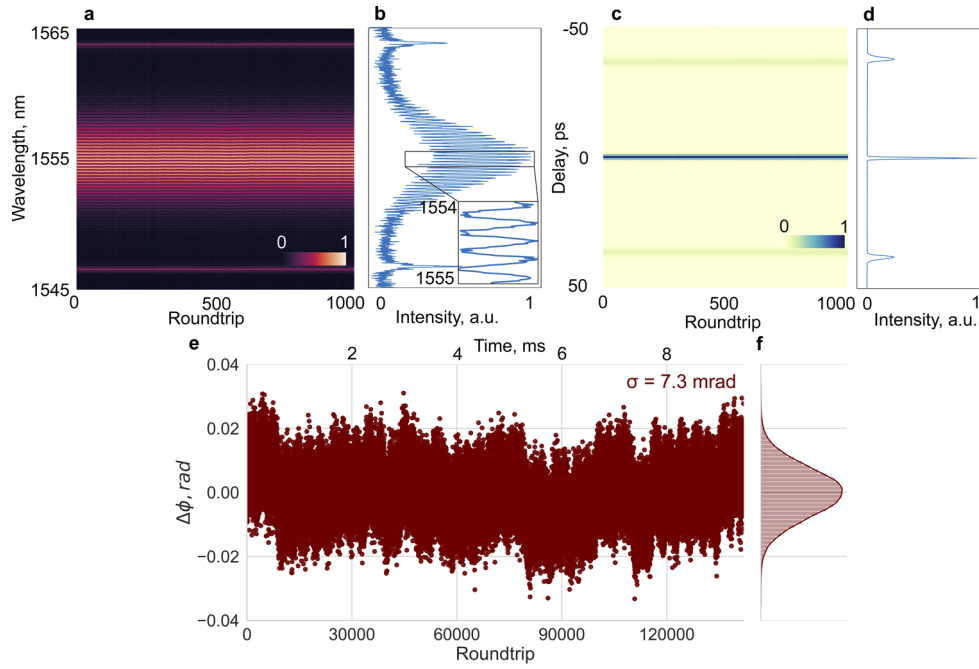
Fig. 2. (**a**) Measured DFT spectra and (**c**) corresponding autocorrelation function. Cross-section of (**b**) the DFT spectra and (**d**) the autocorrelation function. (**e**) Relative phase dynamics in Mach-Zehnder interferometer with equal arms length (excluding the fluctuation of the f_{CEO}) with (**f**) corresponding probability density function.
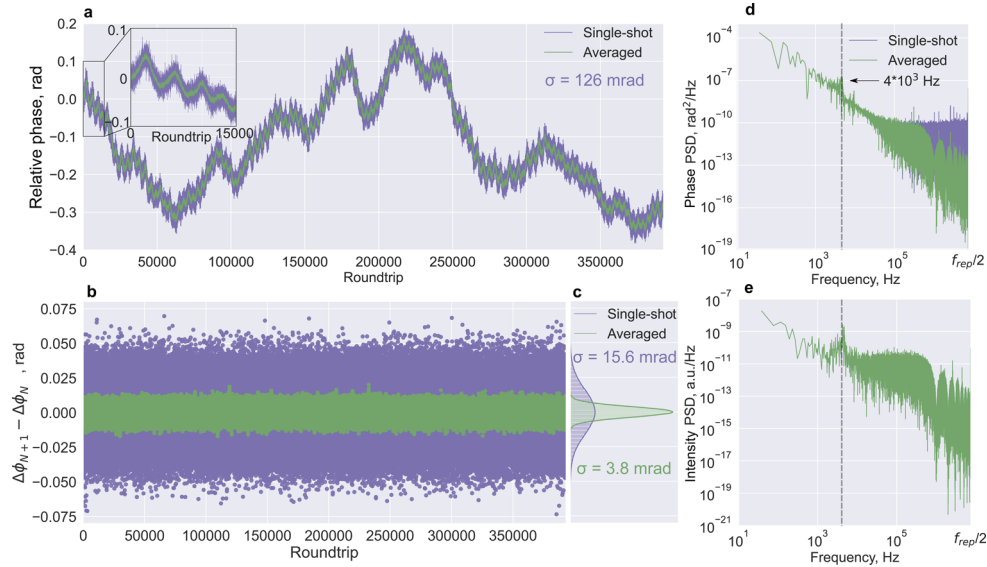

Fig. 3. (**a**) Relative phase drift with standard deviation of 126 mrad. Inset: crop of the fist 15000 roundtrips that illustrates the phase oscillation of the pulse. (**b**) Pulse-to-pulse phase deviation with (**c**) probability density function. Power spectral density (PSD) of (**d**) the phase evolution and (**e**) the pulse intensity with indication of frequencies responsible for phase oscillations. All figures: violet - single shot; green - averaged with a moving window of 15 roundtrips.

averaged values allows further increasing the sensitivity of the setup at a price of a reduced data frequency.

To evaluate the suitability of the proposed method for sensing applications, we recorded the phase dynamics experienced by the laser under vibration exposure. First, the laser was placed on a circular platform, highly sensitive to mechanical vibrations. The vibrations were implemented as a soft mechanical shock in the plane perpendicular to the platform. Figure 4(a) demonstrates a phase evolution of the output pulses during vibration exposure on the laser platform. The pulses show a substantial increase in phase fluctuations with the beginning of vibrations, observed after $50^{t}h$ thousand round trip of recorded evolution. The standard deviation of the complete relative phase evolution increased to 430 mrad. The probability density function, depicted in Fig. 4(b), demonstrates an increase of the standard deviation of the averaged pulse-to-pulse phase slip when using a moving average window of 15 round trips, to 5.5 mrad (Fig. 3(c)). Figure 4(d) shows phase PSD, where oscillation frequencies due to vibrations are clearly distinguished at around 2.5 kHz. These observations confirm that the proposed technique is responsive to vibration exposures and can be successfully used as a platform for sensing application with high acquisition rates.
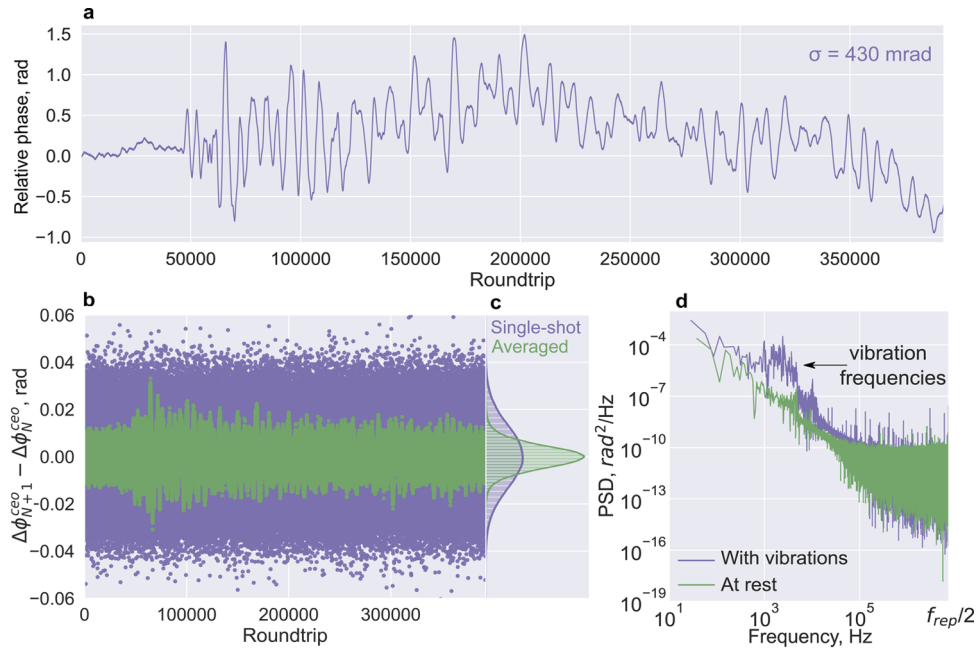

Fig. 4. (**a**) Single-shot relative phase drift under vibration exposure with a standard deviation of 430 mrad. (**b**) Pulse-to-pulse phase deviation of single-shot measurements (magenta) and averaged with a moving window of 15 roundtrips (green) with (**c**) corresponding probability density function. (**d**) Power spectral density of the phase evolution during vibration exposure with an indication of vibration frequencies and at rest (green).

4. Discussion

In this work, we have demonstrated a novel technique in the simple setup, which is able to characterise the pulse-to-pulse stability of the CEO phase with the data frequency of ~15 MHz. This method allowed observing weak oscillations at 4 kHz of the output pulse phase that refers to fluctuations in the pulse energy mediated by the gain medium dynamics or instabilities of the pump laser. This method, based on recording single-shot spectra using DFT, provides ~40 times more accurate measurements than a similar approach, based on the spectrally and spatially

resolved interferometry [30]. Moreover, this technique inherits several advantages compared to the most established methods for CEO phase characterisation, including much higher data rates, a simple linear setup with no limitations to input peak power or pulse duration. Besides, this method could be successfully expanded for other types of ultrashort pulses, since the underlying physics and numerical approach remain the same (e.g. soliton molecules [16,32]).

The current proof-of-principle measurement demonstration has revealed the ambiguity in the reference level of the absolute phase. As was discussed, one of the possible approaches to eliminate such limitation of the measurements is to implement a dispersionless delay line in the Mach-Zehnder interferometer [29], *e.g.* by using hollow-core fibre, preserving all-fibre configuration of the setup. Another approach presents the combination of the proposed method and one of the traditional methods of CEO measurements, such as f-2f interferometer or ATI. While the traditional technique can unambiguously determine the reference level and provide measurements at a longer time scale, the DFT-based technique can characterise pulse-to-pulse dynamics of the CEO phase with MHz data frequency. Increased data rates and single-shot measurements are crucial for investigation of field-driven dynamics in atoms [36], ion-ion coincidence imaging [37,38], time-resolved photo-electron spectroscopy [39]. Additionally, the presented method allows a simple realisation of the cross-interference between two pulse trains, where the first laser is stabilised and serves as a reference level for the second laser or when the second laser is under investigation.

In this work, we also demonstrated the sensing capability of the proposed method. The method has successfully detected vibrations applied to the laser cavity in the kHz frequency range. The proposed technique could also be further optimised for accurate measurements of all parameters underlined in the interference pattern. Thus, the pulse separation information can also be derived from the interference pattern that directly defines the time jitter between consecutive pulses. Importantly, the resolution of the method can be further increased by increasing the DFT resolution [8] or increasing the signal-to-noise ratio via amplified-DFT [40]. An additional increase of the sensitivity can be achieved by suppressing noise by averaging over longer round trip windrows. However, such improvement in sensitivity would come at a price of reduced data acquisition frequency. Maintaining the all-fibre setup, a temperature-insensitive fibre interferometer can be used to eliminate the temperature fluctuations in the long-term operation [41].

We believe that the proposed method has a great potential to pave a novel avenue for phase-based applications at high data rates, including but not limited to high-field physics, biosensing, imaging and optical coherence tomography.

References

1. P. Kozma, F. Kehl, E. Ehrentreich-Förster, C. Stamm, and F. F. Bier, "Integrated planar optical waveguide interferometer biosensors: A comparative review," Biosens. Bioelectron. **58**, 287–307 (2014).
2. V. Giovannetti, S. Lloyd, and L. Maccone, "Advances in quantum metrology," Nat. Photonics **5**(4), 222–229 (2011).
3. T. Lim, Y. Zhou, Y. Lin, Y. Yip, and Y. Lam, "Fiber optic acoustic hydrophone with double mach–zehnder interferometers for optical path length compensation," Opt. Commun. **159**(4-6), 301–308 (1999).
4. R. Abuter, M. Accardo, A. Amorim, N. Anugu, G. Avila, N. Azouaoui, M. Benisty, J.-P. Berger, N. Blind, and H. Bonnet, *et al.*, "First light for gravity: Phase referencing optical interferometry for the very large telescope interferometer," A&A **602**, A94 (2017).
5. V. Wong and I. A. Walmsley, "Analysis of ultrashort pulse-shape measurement using linear interferometers," Opt. Lett. **19**(4), 287–289 (1994).
6. C. Iaconis and I. A. Walmsley, "Spectral phase interferometry for direct electric-field reconstruction of ultrashort optical pulses," Opt. Lett. **23**(10), 792–794 (1998).
7. A. Mahjoubfar, D. V. Churkin, S. Barland, N. Broderick, S. K. Turitsyn, and B. Jalali, "Time stretch and its applications," Nat. Photonics **11**(6), 341–351 (2017).
8. K. Goda and B. Jalali, "Dispersive fourier transformation for fast continuous single-shot measurements," Nat. Photonics **7**(2), 102–112 (2013).

9. G. Herink, B. Jalali, C. Ropers, and D. Solli, "Resolving the build-up of femtosecond mode-locking with single-shot spectroscopy at 90 mhz frame rate," Nat. Photonics **10**(5), 321–326 (2016).

10. J. Peng, M. Sorokina, S. Sugavanam, N. Tarasov, D. V. Churkin, S. K. Turitsyn, and H. Zeng, "Real-time observation of dissipative soliton formation in nonlinear polarization rotation mode-locked fibre lasers," Commun. Phys. **1**(1), 20 (2018).

11. X. Liu, X. Yao, and Y. Cui, "Real-time observation of the buildup of soliton molecules," Phys. Rev. Lett. **121**(2), 023905 (2018).

12. I. Kudelin, S. Sugavanam, and M. Chernysheva, "Build-up dynamics in bidirectional soliton fiber lasers," Photonics Res. **8**(6), 776–780 (2020).

13. I. Kudelin, S. Sugavanam, and M. Chernysheva, "Pulse-onset dynamics in a bidirectional mode-locked fibre laser via instabilities," Commun. Phys. **3**(1), 202 (2020).

14. J. Peng, S. Boscolo, Z. Zhao, and H. Zeng, "Breathing dissipative solitons in mode-locked fiber lasers," Sci. Adv. **5**(11), eaax1110 (2019).

15. C. Lapre, C. Billet, F. Meng, P. Ryczkowski, T. Sylvestre, C. Finot, G. Genty, and J. M. Dudley, "Real-time characterization of spectral instabilities in a mode-locked fibre laser exhibiting soliton-similariton dynamics," Sci. Rep. **9**(1), 13950 (2019).

16. G. Herink, F. Kurtz, B. Jalali, D. Solli, and C. Ropers, "Real-time spectral interferometry probes the internal dynamics of femtosecond soliton molecules," Science **356**(6333), 50–54 (2017).

17. A. Mahjoubfar, K. Goda, A. Ayazi, A. Fard, S. H. Kim, and B. Jalali, "High-speed nanometer-resolved imaging vibrometer and velocimeter," Appl. Phys. Lett. **98**(10), 101107 (2011).

18. T. Xian, L. Zhan, W. Zhang, W. Zhang, and L. Gao, "Single-shot detection time-stretched interferometer with attosecond precision," in *2020 Optical Fiber Communications Conference and Exhibition (OFC)*, (IEEE, 2020), pp. 1–3.

19. M. Chernysheva, S. Sugavanam, and S. Turitsyn, "Real-time observation of the optical sagnac effect in ultrafast bidirectional fibre lasers," APL Photonics **5**(1), 016104 (2020).

20. A. Tikan, S. Bielawski, C. Szwaj, S. Randoux, and P. Suret, "Single-shot measurement of phase and amplitude by using a heterodyne time-lens system and ultrafast digital time-holography," Nat. Photonics **12**(4), 228–234 (2018).

21. P. Ryczkowski, M. Närhi, C. Billet, J.-M. Merolla, G. Genty, and J. M. Dudley, "Real-time full-field characterization of transient dissipative soliton dynamics in a mode-locked laser," Nat. Photonics **12**(4), 221–227 (2018).

22. D. J. Jones, S. A. Diddams, J. K. Ranka, A. Stentz, R. S. Windeler, J. L. Hall, and S. T. Cundiff, "Carrier-envelope phase control of femtosecond mode-locked lasers and direct optical frequency synthesis," Science **288**(5466), 635–639 (2000).

23. S. T. Cundiff, "Phase stabilization of ultrashort optical pulses," J. Phys. D: Appl. Phys. **35**(8), R43–R59 (2002).

24. G. Paulus, F. Grasbon, H. Walther, P. Villoresi, M. Nisoli, S. Stagira, E. Priori, and S. De Silvestri, "Absolute-phase phenomena in photoionization with few-cycle laser pulses," Nature **414**(6860), 182–184 (2001).

25. M. C. Stowe, F. C. Cruz, A. Marian, and J. Ye, "High resolution atomic coherent control via spectral phase manipulation of an optical frequency comb," Phys. Rev. Lett. **96**(15), 153001 (2006).

26. D. Hoff, F. J. Furch, T. Witting, K. Rühle, D. Adolph, A. M. Sayler, M. J. Vrakking, G. G. Paulus, and C. P. Schulz, "Continuous every-single-shot carrier-envelope phase measurement and control at 100 khz," Opt. Lett. **43**(16), 3850–3853 (2018).

27. M. Natile, A. Golinelli, L. Lavenu, F. Guichard, M. Hanna, Y. Zaouter, R. Chiche, X. Chen, J. Hergott, W. Boutu, H. Merdji, and P. Georges, "Cep-stable high-energy ytterbium-doped fiber amplifier," Opt. Lett. **44**(16), 3909–3912 (2019).

28. M. Kurucz, S. Tóth, R. Flender, L. Haizer, B. Kiss, B. Persielle, and E. Cormier, "Single-shot cep drift measurement at arbitrary repetition rate based on dispersive fourier transform," Opt. Express **27**(9), 13387–13399 (2019).

29. L. Xu, C. Spielmann, A. Poppe, T. Brabec, F. Krausz, and T. W. Hänsch, "Route to phase control of ultrashort light pulses," Opt. Lett. **21**(24), 2008–2010 (1996).

30. K. Osvay, M. Görbe, C. Grebing, and G. Steinmeyer, "Bandwidth-independent linear method for detection of the carrier-envelope offset phase," Opt. Lett. **32**(21), 3095–3097 (2007).

31. M. Chernysheva, M. Al Araimi, H. Kbashi, R. Arif, S. V. Sergeyev, and A. Rozhin, "Isolator-free switchable uni-and bidirectional hybrid mode-locked erbium-doped fiber laser," Opt. Express **24**(14), 15721–15729 (2016).

32. Z. Wang, K. Nithyanandan, A. Coillet, P. Tchofo-Dinda, and P. Grelu, "Optical soliton molecular complexes in a passively mode-locked fibre laser," Nat. Commun. **10**(1), 830 (2019).

33. J. Kim and Y. Song, "Ultralow-noise mode-locked fiber lasers and frequency combs: principles, status, and applications," Adv. Opt. Photonics **8**(3), 465–540 (2016).

34. R. Paschotta, "Noise of mode-locked lasers (part ii): timing jitter and other fluctuations," Appl. Phys. B **79**(2), 163–173 (2004).

35. K. Wu, P. P. Shum, S. Aditya, C. Ouyang, J. H. Wong, H. Q. Lam, and K. E. K. Lee, "Noise conversion from pump to the passively mode-locked fiber lasers at 1.5 μm," Opt. Lett. **37**(11), 1901–1903 (2012).

36. M. S. Schöffler, X. Xie, P. Wustelt, M. Möller, S. Roither, D. Kartashov, A. M. Sayler, A. Baltuska, G. G. Paulus, and M. Kitzler, "Laser-subcycle control of sequential double-ionization dynamics of helium," Phys. Rev. A **93**(6), 063421 (2016).

37. J. Ullrich, R. Moshammer, A. Dorn, R. Dörner, L. P. H. Schmidt, and H. Schmidt-Böcking, "Recoil-ion and electron momentum spectroscopy: reaction-microscopes," Rep. Prog. Phys. **66**(9), 1463–1545 (2003).

38. J. Long, F. J. Furch, J. Durá, A. S. Tremsin, J. Vallerga, C. P. Schulz, A. Rouzée, and M. J. Vrakking, "Ion-ion coincidence imaging at high event rate using an in-vacuum pixel detector," J. Chem. Phys. **147**(1), 013919 (2017).

39. M. I. Stockman, M. F. Kling, U. Kleineberg, and F. Krausz, "Attosecond nanoplasmonic-field microscope," Nat. Photonics **1**(9), 539–544 (2007).

40. K. Goda, D. R. Solli, K. K. Tsia, and B. Jalali, "Theory of amplified dispersive fourier transformation," Phys. Rev. A **80**(4), 043821 (2009).

41. W. Zhu, E. R. N. Fokoua, Y. Chen, T. Bradley, M. N. Petrovich, F. Poletti, M. Zhao, D. J. Richardson, and R. Slavík, "Temperature insensitive fiber interferometry," Opt. Lett. **44**(11), 2768–2770 (2019).